Available online at www.sciencedirect.com

SCIENCE DIRECT®

Vision Research 44 (2004) 103–112

Vision Research

www.elsevier.com/locate/visres

The multifocal pattern electroretinogram in glaucoma ☆

Sandra Stiefelmeyer [a], Aljoscha S. Neubauer [a,*], Thomas Berninger [a], Geoffrey B. Arden [b], Günther Rudolph [a]

[a] *Department of Ophthalmology, Ludwig-Maximilians-Universität, Mathildenstrasse 8, 80336 Muenchen, Germany*

[b] *Applied Vision Research Centre, Department of Optometry and Visual Science, City University, 311 Goswell Road, London EC1 V 7DD, UK*

Received 12 June 2002; received in revised form 29 July 2003

Abstract

Background: The pattern ERG can be used to detect early glaucomatous change, because the response of cells in the inner retina from (typically) 20°–40° of area is reduced before perimetric abnormality is certain. The multifocal pattern electroretinogram (mfPERG) allows analysis of many local regions within this area. The aim of this study was to investigate whether in patients with presumed glaucoma the mfPERG permits diagnosis and discrimination from normals.

Methods: Measurements on 25 age-related normal eyes were compared to those on 23 eyes with different stages of glaucoma. A RETIScan system was used to generate a stimulus pattern of 19 hexagons, each consisting of six triangles. The triangles pattern-reversed black to white at 75 Hz. Those 19 hexagons were grouped into three stimulus regions: a central field, a middle, and a peripheral ring. The complete array subtended 48° at the eye. The hexagons alternated between black and white, in a temporal pattern that followed a corrected binary *m*-sequence (length 512, 10 cycles with 39 s each). The amplitudes and latencies of positive responses at approximately 50 ms (P-50) and negative responses at approximately 95 ms (N-95) were analyzed.

Results: In patients with glaucoma the P-50 and N-95 components of the mfPERG were significantly reduced for the central area and both outer rings compared to normal volunteers ($p < 0.001$, Mann–Whitney-*U*). The most distinct reduction was observed for N-95 and the central ring. Changes in latencies were not conclusive. The reduction of the components increased with the stage of glaucoma. A predictive model for detecting early glaucomatous changes was designed based on P-50–N-95 with 88% sensitivity and 76% specificity.

Conclusion: In glaucoma a marked reduction of components, especially centrally is observed in the mfPERG. This hints to an early involvement of central ganglion cells and may be useful for future functional tests.

Keywords: Glaucoma; Multifocal pattern ERG

1. Introduction

Visual loss in chronic glaucoma results from destruction of retinal ganglion cells. However, visual field loss occurs relatively late in the progression of this disease. Estimations suggest that at least 25–35% of the ganglion cells must be lost prior to the development of a field abnormality detectable with modern automated threshold visual field testing (Kerrigan-Baumrind, Quigley, Pearse, Kerrigan, & Mitchell, 2000). As a result there still is considerable interest in developing more sensitive and more reliable methods for making an earlier diagnosis in glaucoma.

A non-invasive, fast method for studying the pathogenesis and pathophysiology of retinal ganglion cell damage is provided by the pattern electroretinogram (PERG) first described in 1964 by Riggs, Johnson, and Schick. Currently the domain of standardized PERG is the diagnosis of generalized disease of ganglion cell dysfunction (Groneberg & Treping, 1980; Holder, 2001; Maffei & Fiorentini, 1981; Sieving & Steinberg, 1987; Zrenner, Baker, Hess, & Olsen, 1987). It has also been applied to detect and follow changes in glaucoma (Bach, 2001; Korth, 1997). Typical changes could be shown, mainly a reduction of amplitudes (Bach, Pfeiffer, &

☆ The authors have no proprietary interest in any of the equipments and materials used in this study.

* Corresponding author. Tel.: +49-89-5160-3811; fax: +49-89-5160-5160.

E-mail address: aneubaue@ak-i.med.uni-muenchen.de (A.S. Neubauer).

0042-6989/$ - see front matter © 2003 Elsevier Ltd. All rights reserved.
doi:10.1016/j.visres.2003.08.012

Birkner-Binder, 1993) with the second negative wave being affected most (Weinstein et al., 1988). The observed amplitude reductions allow to some degree to predict the conversion of ocular hypertension to early glaucoma (O'Donaghue et al., 1992; Pfeiffer, Tillmon, & Bach, 1993; Salgarello et al., 1999). Thus the PERG as compared to other functional tests (Bayer, Maag, & Erb, 2002; Graham et al., 1996) seems an efficient diagnostic tool but to date it has not been generally employed. This may be partly explained by the additional testing time necessary for the patient (often located in a separate department). Moreover, PERG testing must compete with other new functional tests such as frequency doubling technology perimetry, which are more easy to perform and may offer even better sensitivities (Bayer & Erb, 2002).

The ordinary, luminance ERG gives no information about the location of retinal damage. The PERG can demonstrate that damage has occurred within the (fairly large) area of the checkerboard used to stimulate the eye (Bach, Sulimma, & Gerling, 1997). However, more localized defects of the visual field are frequently observed in patients with glaucoma. With the introduction of a multi-input stimulus system it became possible to record many local ERG responses from the retina simultaneously (mfERG). Usually the response to change in luminance of many small independent areas is obtained. This method was first introduced by Sutter and Tran (1992) who showed how, if the whole test field was divided into a number of areas in each of which luminance is modulated independently with time, in a pseudorandom manner, it was possible to calculate mfERGs with a simple PC. When applied to glaucomatous changes inhomogeneous results were obtained. No correlation to visual field defects was found in early glaucoma patients in the mfERGs (Fortune, Johnson, & Cioffi, 2001; Hood et al., 2000; Sakemi, Yoshii, & Okisaka, 2002). A selective loss of an oscillatory component could be proven using special multiflash stimulation techniques (Fortune, Bearse, Cioffi, & Johnson, 2002) helpful to differentiate between normal and glaucomatous eyes (Palmowski, Allgayer, Heinemann-Vernaleken, & Ruprecht, 2002).

The recently available multifocal pattern ERG (mfPERG) combines pattern ERG stimulation with the multifocal technique in order to achieve a topographic mapping of the pattern ERG. The response is thought to be developed mainly by ganglion cells. However, it has been found (Klistorner, Graham, & Martins, 2000), that topographic changes to the mfPERG in glaucomatous patients do not correlate well with visual field defects. Part of the pattern response may be developed by other retinal elements—e.g. amacrine cells—and changes in the amplitude of electrical activity may not indicate that function has been lost. This discrepancy raises the question whether the mfPERG technique can contribute to glaucoma diagnosis at all. The aim of this study was to further determine if the mfPERG changes in a characteristic manner in glaucoma patients and permits the diagnosis of an abnormality.

2. Subjects and methods

2.1. Subjects

Twenty-three eyes from 13 patients with open angle (POAG) or low tension glaucoma were included in the study. Each patient had been fully ophthalmologically examined at least three times and had provided at least three visual fields the 30-2 program of Humphrey field analyzer (HFA; Humphrey, San Leandro, CA, USA) at the time of mfPERG testing. Diagnosis of glaucoma was based upon the typical appearance and deterioration of the optical disc, changes to the visual fields and (in POAG) elevated intra-ocular pressure. Informed consent was obtained from each participant. All methods adhered to the Declaration of Helsinki 2000 for research involving human subjects.

Patients with glaucoma had a mean age of 65.8 years with a standard deviation (SD) of 9.63 years (range 42–79 years). Twelve right eyes (OD) and 11 left eyes (OS) were included. Table 1 summarizes the patients. Two graders (SS and ASN) independently performed classification of visual field defects of all eyes using methods established by Aulhorn (Aulhorn & Karmeyer, 1977). The Aulhorn classification distinguishes five stages of visual field defects: stage I shows only relative scotomas. Stage II shows absolute scotomas which do not continue to the blind spot, while in stage III absolute scotomas reach the blind spot. In stage IV more than one quadrant is affected, but the center remains free. In Stage V the visual field is very reduced, with only a temporal isle left. In this study six eyes were graded Aulhorn I, 10 eyes Aulhorn II, 3 eyes Aulhorn III and 4 eyes Aulhorn IV. No patient with Aulhorn stage V was included. Average mean defects (MD) in the four Aulhorn groups were MD ± SD in dB: -5.68 ± 1.92; -6.37 ± 2.64; -13.09 ± 1.92; -17.63 ± 5.83.

Best-corrected visual acuity was 0.5 or better at the time of testing and cup-to-disc ratio was—corresponding to the visual field defects—0.5–1.0 cupping. The patients had no history of diabetes or other systemic disease and no reported ophthalmologic or neurological surgery or other diseases affecting vision.

As a control group we examined 25 age-related normal eyes from 25 healthy individuals. Informed consent was obtained from all participants. The healthy subject ages ranged from 40–72 years, mean 61.63 ± 10.35. Healthy eyes had a measured intra-ocular pressure (IOP) of less than 21 mmHg and no history of elevated IOP. The optic disc appeared healthy based on stereo-

Table 1
Characteristics of glaucoma patients

ID number	Patient initials	Age	Male/ Female	Eye (OD/OS)	Best corrected visual acuity	Ocular tension under therapy (mmHg)	Glaucoma stage (Aulhorn)	Refractive correction for 30 cm distance	Visual field mean deviation (dB)
1	K. B.	72	M	OS	0.5	19	2	+2.75/−1.0/5°	−1.75
2	M. D.	74	M	OD	0.8	15	3	+2.5/0/0°	−15.12
3	W. M.	63	M	OD	0.9	16	2	−0.25°/0/0°	−6.49
4	W. M.		M	OS	0.7	17	2	−1.25/0/0°	−7.78
5	J. K.	74	M	OD	0.5	18	2	+3.25/−0.5/161°	−7.38
6	J. K.		M	OS	0.9	16	4	+2.5/−0.25/27°	−22.44
7	H. P.	57	F	OD	0.6	13	1	+3.75/−0.25/170°	−6.99
8	H. P.		F	OS	0.7	13	2	+4.25/−0.5/180°	−7.87
9	I. R.	60	F	OD	0.8	24	2	+4.25/−1.0/146°	−9.22
10	I. R.		F	OS	1.0	22	1	+4.75/−1.0/70°	−5.08
11	K. R	66	M	OD	0.5	18	4	+3.75/−0.25/130°	−9.95
12	K. R		M	OS	1.0	21	4	+3.75/−0.75/165°	−16.27
13	R. S.	67	F	OD	0.8	9	4	+3.0/−0.5/135°	−21.86
14	R. S.		F	OS	0.9	13	2	+3.25/−0.5/70°	−8.08
15	G. S.	79	F	OD	0.7	21	3	+3.75/−0.75/75°	−12.83
16	G. S.		F	OS	0.7	21	3	+2.5/−0.75/70°	−11.31
17	M. S.	71	F	OD	0.6	16	2	+3.0/−0.5/90°	−1.42
18	K. S.	60	M	OD	0.8	14	1	+2.25/−4.0/179°	−3.19
19	K. S.		M	OS	1.0	14	2	+2.0/−2.25/176°	−7.04
20	B. W.	70	F	OD	0.5	16	1	+2.5/−0.25/89°	−7.49
21	B. W.		F	OS	0.9	16	2	+2.0/−0.5/130°	−6.64
22	S. Z.	42	F	OD	1.0	16	1	+1.25/−0.75/45°	−3.82
23	S. Z.		F	OS	1.0	17	1	+1.25/−1.0/5°	−7.51

scopic fundus exam with the biomicroscope with an overall cup to disc ratio of <0.4. No history of any chronic eye disease or previous ocular surgery was present. Visual acuity for normal volunteers was 1.0 or better with correction.

2.2. Stimulation

To perform the mfPERG measurements, a RETIScan System (Roland Consult, Wiesbaden, Germany) was used. A stimulus pattern of 19 patterned hexagons, each consisting of six triangles (alternately black and white) was used. The stimulus was presented on a 21-inch monitor viewed at 30 cm distance within a central 48° total visual field (visual angle of 24°). No scaling factor was used, which means that the central hexagon (macula) had the same size (9.6° visual field) as the peripheral hexagons. Mean luminance of the stimulus on the monitor was 180 cd/cm^2. Each hexagon element changed in time between black and white (contrast was approximately 98%) following a binary *m*-sequence. Each hexagon was modulated at the frequency of 75 Hz with an on/off-probability of 0.5 (Bearse & Sutter, 1996; Sutter & Bearse, 1999). The traces produced by the computational procedure were smoothed by an algorithm within the software (Retiscan version 3.15). It consisted of 3–5 times smoothing and additional band pass filtering between 10 and 100 Hz. The number of smoothings necessary was chosen by the examiner, but did not exceed 5.

2.3. Recording and response analysis

Patients were refracted and addition lenses given so the screen was in sharp focus, despite any presbyopia. A red fixation target of 2 cm diameter was placed in the center of the stimulus. For all recordings loop electrodes were used (AVANTA, Lubljana, Slovenia). The reference electrodes were at the temple and the ground electrodes at the forehead. The conjunctiva was anaesthetized with oxybuprocain 0.4% eye drops. The pupil size was 3–4 mm in all patients and normal subjects. Room illumination was always the same and no miotic or mydriatic eye drops were given. Fixation was equal in patients and normals and was manually controlled by the operator during measurements. If any decentration of the pupil relatively to the fixation target was noted, data acquisition was interrupted and the patient asked to fixate.

The pattern changed in accordance to the structure of a corrected *m*-sequence (Sutter & Tran, 1992). Duration of data acquisition was approximately 6.5 min with a length of 512 divided into 10 sessions of 39 s each. The signals were band pass-filtered with a high cut at 100 Hz and a low cut at 10 Hz. By cross-correlation analysis between stimulation patterns and their responses 19 focal mfPERGs can be displayed, and in the figures are shown in their relative topographical positions. For further analysis the responses were grouped into three ring regions (see Fig. 1B and D): a central hexagon (macula, no. 10 in Fig. 1), a middle (nos. 5, 6, 9, 11, 14,

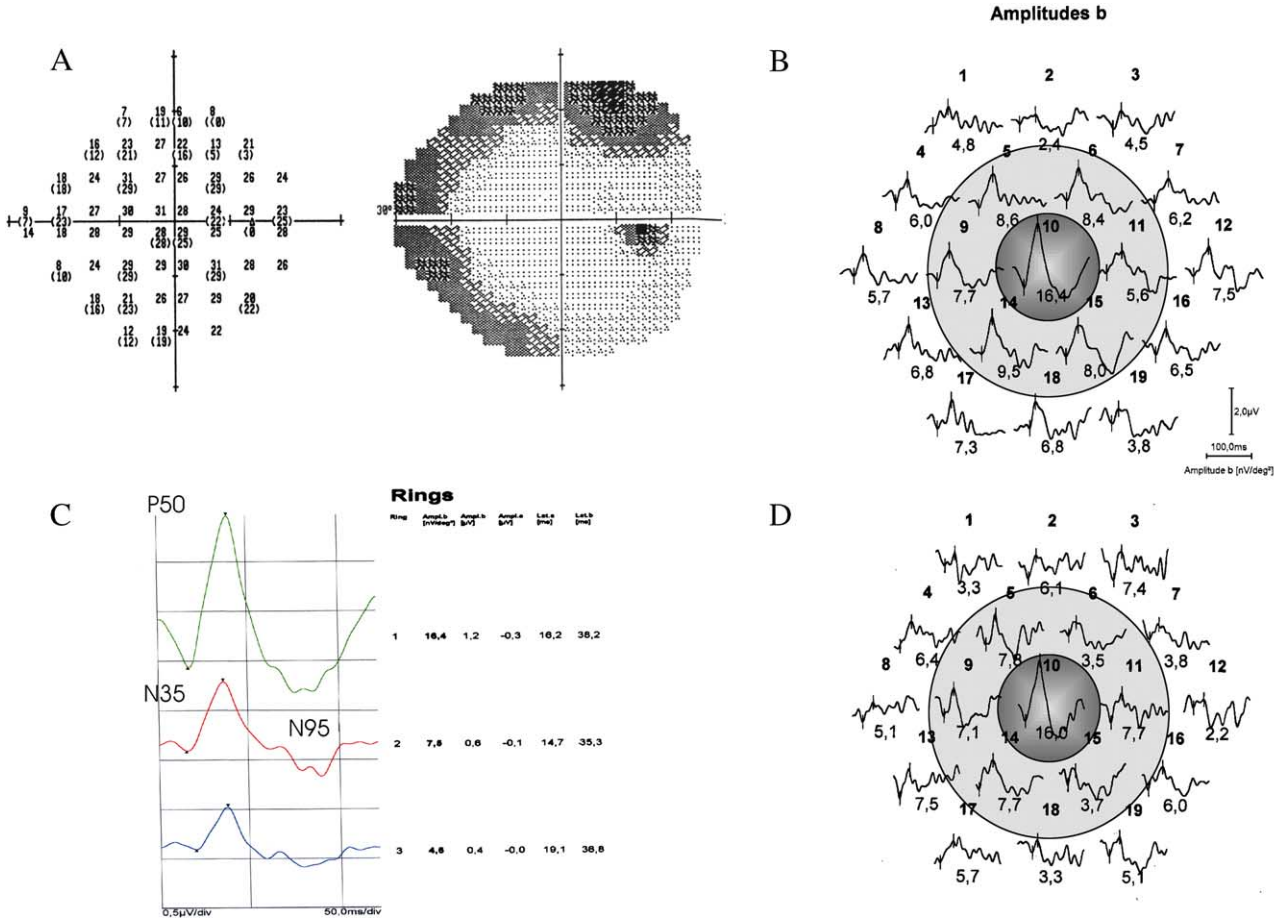

Fig. 1. (A–D) mfPERG of a glaucoma patient, whose visual field defect is graded Aulhorn 1 (A–C) compared to an age-matched control (D). The visual field in (A) shows the patient's temporal relative scotoma. The 19 multifocally measured PERG amplitudes P-50 are shown below for this glaucoma patient (B). One can see a slight temporal decrease in amplitude corresponding to the visual field defect. The summed responses are plotted in (C). However, an overlap with normal controls exists, as shown in the very similar responses from an age-matched control. (D) No differences in latencies or curve forms were found.

15 in Fig. 1) and peripheral ring (remaining numbers in Fig. 1). Each of the two rings represents an averaged response from several hexagons (Fig. 1C). Decreasing amplitude was seen over the three regions, the periphery giving smallest responses (Fig. 1C). The central region essentially gives the response of the macula, the middle ring the response of the perimacular area, and the peripheral ring that of the mid-periphery.

For each mfPERG a positive component at approximately 50 ms (P-50) and a negative component at approximately 95 ms (N-95) can be seen. The P-50 often rises from a still earlier negative wave. The positive component is measured from this trough to the following positive peak of P-50. The following negative N-95 component is measured from the peak of P-50 to the following trough at approximately 95 ms (Fig. 1C). Peaks were identified manually in the each of the single plots by the minimum respectively maximum value (close to the expected latency). Identification is usually clearer in the single plots than in the summarized curves, which markers were automatically transferred to by the software. Latencies in milliseconds (ms) were also measured and analyzed for every ring for the positive and negative components in the same manner. The latencies of the first trough, of P-50 and N-95 were investigated.

2.4. Data analysis

Data were collected and analyzed using SPSS 10.0 for Windows (SPSS Inc., Chicago, IL, USA). On all tests used, $p < 0.05$ was considered significant. Unless other specified for comparisons of mean the non-parametric Mann–Whitney-U test was used. For all linear regressions calculated 95% confidence intervals are given. To identify possible significant factors a comprehensive graphical analysis of all results was performed using scatterplots and boxplots. Receiver operational characteristic (ROC) curves were calculated with SPSS 10.0.

3. Results

3.1. Group differences between normals and glaucoma patients

First, differences between the control group and all glaucomatous eyes were investigated. The mfPERGs were analyzed for significant changes in amplitudes of the positive P-50 and negative N-95 and for changes in the latencies of the first trough, of P-50 and N-95. The results are summarized in Fig. 2. The boxes shown represent the 25th and 75th percentiles, the line in the box is the median (i.e. the 50th percentile). The "whiskers" show the 10th to 90th percentiles. The small circles mark single values lying outside this range. It can be seen in Fig. 2, that the positive P-50 as well as the negative N-95 component was highly significantly reduced for every region in patients with glaucoma ($p < 0.001$). The relative reduction was higher in the central region than in the 1st and 2nd ring and the reduction was even more distinct for the negative components. In normals linear regression analysis showed no significant change in thresholds with age ($p > 0.9$). The same is true for patients with glaucoma.

Analysis of latencies showed inconclusive results. No significant effect could be observed for the latency of N-95 and P-50. Only the latency of the first trough was slightly increased in ring 2 ($p = 0.025$). Therefore, further data for latencies are not shown.

3.2. Changes in mfPERG correlates to Aulhorn stage

The correlation of Aulhorn stage and the mean defect (MD) in automated perimetry was significantly high (Spearman's Rho $= -0.751$, $p < 0.001$). As the same results were obtained by each grading method, only Aulhorn stages are shown in the analysis. In Fig. 3 a clear reduction of amplitudes for N-95 with progressive glaucomatous damage is observed. A relatively large central reduction with early glaucoma stages Aulhorn 1 and 2 existed, while only slight changes were observed for stages higher than Aulhorn 2. Throughout the study even for advanced absolute scotomas no topographic correlation of local amplitudes and localized visual field defects could be shown.

A linear regression analysis was performed, to quantify the degree of reduction of P-50 and N-95 with the Aulhorn stage. The model was $Y = mX + C$, where $Y =$ mfPERG voltage in [nV], $X =$ Aulhorn stage and $C =$ regression constant. For P-50 of the central region the factor m was -2.38 with a 95% confidence interval of $[-3.04; -1.72]$. The constant C was 15.99 nV, with a 95% confidence interval of [15.10; 16.88]. Both regression factors were highly significant at $p < 0.001$ (R^2 of the regression line was 0.42). Linear regression for the negative component N-95 for the central region resulted in a factor m of -2.76 with a 95% confidence interval $[-3.79; -1.72]$. The constant C here was 21.61 nV, confidence interval [20.21; 23.01]. Again, both regression factors were highly significant at $p < 0.001$ and R^2 of the regression line was 0.28.

Regarding latencies linear regression models did not yield any significant regression coefficients m for the latency of the first trough ($p > 0.1$) for all retinal regions. The coefficients calculated for the slightly increasing latency of P-50 for the central region and ring 2 and for the slightly increasing latency of N-95 for the central region only (non-standardized beta $= 2.49$,

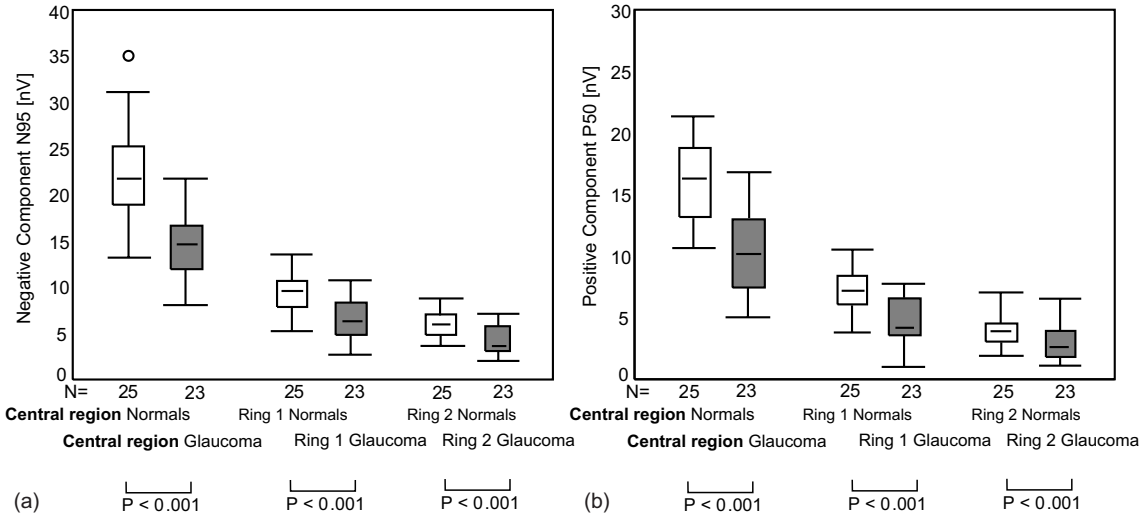

Fig. 2. (a,b) Amplitudes of mfPERG components in normal and glaucoma patients. In (a) a decrease of the negative component N-95 towards the periphery is seen. Amplitudes of N-95 are significantly reduced for glaucoma patients in all rings (a). The boxes represent the 25th and 75th percentiles, the line in the box is the median (i.e. the 50th percentile). The "whiskers" range from the 10th to 90th percentiles. The small circles mark single values lying outside this range. A similar reduction is observed for the positive component P-50 (b).

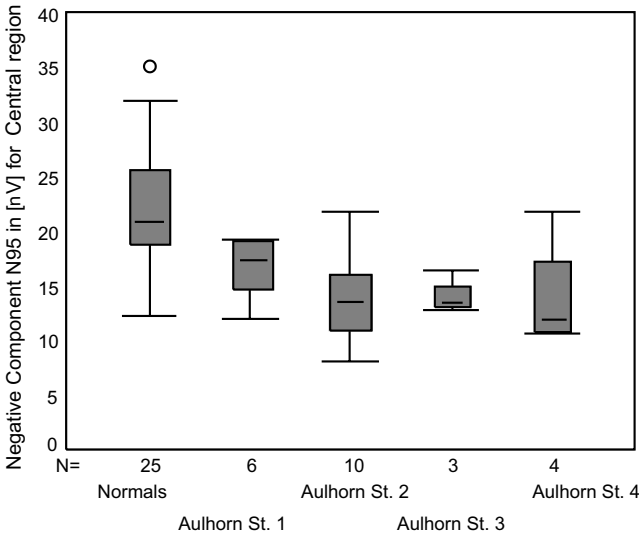

Fig. 3. Characteristic change of components in different stages of glaucoma. A reduction of all components—most markedly in N-95 of the central region—can be seen in glaucoma patients. There is a relatively large central reduction in early glaucoma, while only further slight changes are observed for stages higher than Aulhorn 2. For a detailed description of the boxplots see Fig. 2.

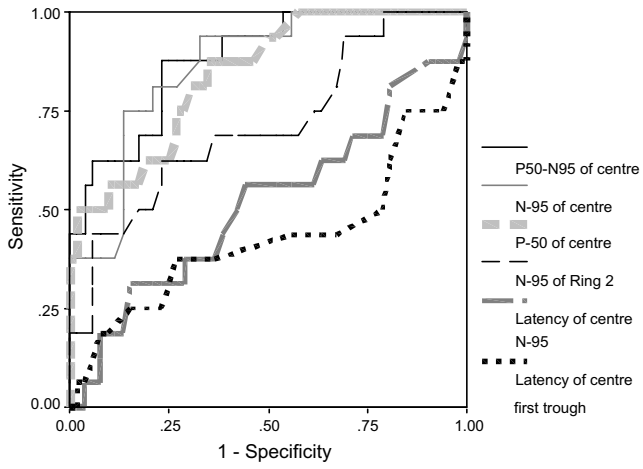

Fig. 4. ROC curve for different mfPERG parameters. Best area under the curve is obtained for P-50–N-95 yielding a sensitivity of 88% with a specificity of 77%. The other amplitudes also show acceptable ROC curves. Best ROC curves for latencies are also shown, but they yield characteristics inacceptable for designing a diagnostic test for glaucoma.

$p = 0.015$) were, however, significant. In summary an slight increase in all latencies could be observed when glaucoma stages proceeded. In contrast, when comparing early stage 1 glaucoma patients and normal patients, a slight decrease was seen in early glaucoma patients for all latencies. This effect remained non-significant for all latencies tested but for the latency of N-95 in ring 2 ($p < 0.001$; Mann–Whitney U test).

3.3. Predictive model for glaucoma detection

In order to develop a predictive model for screening for early stages of glaucoma the Aulhorn stages 1 and 2 were considered as early glaucoma stages. A total of 16 glaucomatous eyes and 25 normal eyes were available for modeling. ROC analysis of all components and latencies revealed that a reduction of amplitude was a stronger predictor than a shortening of latency. In Fig. 4 typical ROC curves are given. Maximal area under the normalized ROC curve (area ± SEM) for P-50–N-95 was 0.86 ± 0.05. For the single parameter N-95 of the central region a ROC area of 0.84 ± 0.05 was achieved. Good ROC characteristics were also obtained with P-50 of the central region (0.83 ± 0.05). Lesser, though highly significant values were found for other data sets, e.g. N-95 in ring 2 (0.72 ± 0.08). Only the best two ROC curves with latencies are shown in Fig. 4. Latency for N-95 of the central region yielded 0.51 ± 0.09 ROC area and latency of the first trough of the central region gave 0.43 ± 0.10.

In these results, the limiting value of P-50–N-95 was 31.6 nV. This gave an optimal sensitivity and specificity of 88% and 76% respectively. When using the best ROC based on latencies, i.e. latency of N-95 for the central region, a sensitivity of 90% yielded 0% specificity thus making further analysis useless. Other descriptive constructs such as the ratio of peak/trough and relative latencies did not yield any significant results and therefore are not shown here.

4. Discussion

4.1. Reduction of components in glaucoma

The mfPERG allows determination of local dysfunction of ganglion cells and very small macular lesions can be detected with the identical instrument used here (Kretschmann, Bock, Gockeln, & Zrenner, 2000). It thus provides a means to analyze regional variations in nerve fiber layer dysfunction as is known from nerve dissection experiments (Vaegen, Anderton, & Millar, 2000). In glaucoma—besides loss of ganglion cell function, it has recently been shown that outer retinal pathology occurs (Raz et al., 2002; Velten, Korth, & Horn, 2001) especially in the peripheral retina. Our results show a significant reduction in all regions regarding positive and negative components. In early stages the fovea should theoretically be less affected. Our results, however, show in agreement with the findings of Chan and Brown for the mfERG (1999, 2000), a relative reduction in all regions involving the central rings even more than the peripheral rings.

There is therefore a discrepancy between the results of field testing, that show the earliest glaucomatous changes peripherally, in the Bjerrum region, and usually

in one quadrant, and the results from mfPERG. One possible reason is that the better results on mfPERG testing in the central zone, as shown by the ROC curves, is due to the better signal to noise ratio obtained from the larger responses in the center. While this may in part be true, the results shown in Fig. 2 suggest that it cannot be the entire story. Indeed, even if the abnormality was no greater in the central zone than in the periphery, this would still conflict with the results of field testing. We do not know why exactly the PERG or mfPERG is reduced in glaucoma in macular regions which are only shown to be abnormal by field testing in end-stage disease. However the discrepancy could imply that there is inner retinal damage which is more widespread and more uniform than field tests suggest. This view is supported by animal experimental data where in ocular hypertensive primates a similar degree of ganglion cell loss in the central and peripheral retina was observed (Hare et al., 2001).

In the central region the ratio of ganglion cells to photoreceptors is higher than in the periphery (Curcio, Sloan, Packer, Hendrickson, & Kalina, 1987; Esterberg, 1935) reducing from 1:4 in the center to 1:1 at about 15° (Wassle, Grunert, Rohrenbeck, & Boycott, 1989), and the overlap between receptive fields may be higher. Therefore when an equal proportion of ganglion cell signals are abnormal in all the retina, the defect may be most obvious on visual field testing in the periphery. Thus the mfPERG results may explain clinical features of glaucoma which have hitherto been puzzling. Morphological data obtained by optical coherence tomography (Greenfield, Bagga, & Knighton, 2003; Guedes et al., 2003) and the retinal thickness analyzer (Asrani et al., 2003) support a marked involvement of the macula in the early phases of glaucoma. Therefore in the central area a ring-wise analysis has some justification. For the periphery, theoretically other analysis patterns might be advantageous such as quadrant testing (Shorstein, Dawson, & Sherwood, 1999). However, no topographic correlation to peripheral visual field defects could be shown in mfPERG testing in agreement with Klistorner et al. (2000). Moreover, the macula is most involved in early glaucoma, as shown in this study and the in in-vivo morphological data described above. Therefore, in contrast to visual field testing it is doubtful if the value of peripheral testing by mfPERG can be improved by different grouping patterns.

4.2. Number of fields

Unlike most other studies—besides not using a scaling factor—we used only 19 fields rather than 61 fields. This may in part also account for that in our study the mfPERG recordings did not show significant alterations with age in contrast to Klistorner et al. (2000) and Lindenberg, Horn, Rühl, and Korth (2001). In preliminary experiments we observed that variability of the responses significantly increased and the stability of results is lost when more than 19 hexagons are used.

4.3. Latencies in glaucoma

Berninger and Arden (1988) have reported the positive and negative latencies of the PERG to be very stable and only rarely changed by diseases. There are only a few reports about a delay of the P-50 PERG latencies (Holder, 1987; Marx, Bodis-Wollner, Lustgarten, & Podos, 1988; Weinstein et al., 1988). In group comparison the glaucoma group did not show consistently altered latencies as compared to normals. Comparing different glaucoma stages, however, a slight increase of latencies with increase of the stage of the disease could be observed. This cannot be explained by increasing age as in Korth, Horn, Strock, and Jonas (1989), as all Aulhorn groups in this study had approximately the same age (see Table 1). The changes in latency may, therefore, be caused by an increase of glaucomatous damage. The amount of the change, however, is very small, which makes latency unsuitable for diagnosing or following glaucoma patients.

4.4. Mechanisms

The early positive and later negative responses of the mfPERG wave are affected differently in diseases and may be generated by different mechanism. It is known, that N-95 is selectively lost in optic neuropathy while P-50 is reduced when ganglion cells and/or their input are involved (Hess & Baker, 1984; Hollander, Bisti, Maffei, & Hebel, 1984). If N-95 alone is involved, the lesion must be localized more centrally in the optic pathway, while good input from the retina can be assumed (Holder, 2001). However, if P-50 is also reduced, this may result from a ganglion cell loss but may also reflect a reduced input from the retina. The exact localization where P-50 is generated is still not known. It is, however, distinctly different from the more ganglion-cell associated N-95 and is reduced in animal models with experimental glaucoma (Holder, 2001; Viswanathan, Frishman, & Robson, 2000).

In the glaucoma patients examined in this study a marked reduction was observed for N-95 as well as for the P-50 components. The theoretically expected topical pattern—i.e. more reduction in the periphery than in the central field—however, could not be observed in agreement with Klistorner et al. (2000). This does not question the usefulness of the mfPERG for early detection of glaucoma. Instead, this divergence of mfPERG results from visual field defects hints to not only peripheral optic nerve fiber defects but also ganglion cell loss and central optic nerve changes occurring in glaucoma. These changes precede the visual field defects.

4.5. Comparison to PERG

In conventional full-field PERG testing a reduction of amplitudes allowing to some degree to predict the conversion of ocular hypertension to early glaucoma has been shown (O'Donaghue et al., 1992; Pfeiffer et al., 1993). The second negative wave appears to be affected most (Weinstein et al., 1988). Regarding localization a generalized reduction in glaucoma was suggested by PERG (Bach et al., 1993), which is supported by our data showing a strong macular involvement in early glaucoma. Conventional PERG testing provides good test characteristics for glaucoma, best for P-50–N-95 yielding 0.78 area under the ROC curve (Bayer et al., 2002; Bayer & Erb, 2002). This is comparable to the 0.86 area under the curve obtained for the multifocal PERG in this study, where also N-95–P-50 gave the best test characteristics. Remarkably, for the mfPERG the macular field was most predictive. This supports the theory that fast glaucoma screening strategies focused of the macula may provide good test characteristics.

4.6. Comparison to mfERG

Several studies have shown a loss of function in glaucomatous damage by using the multifocal ERG (Bearse & Sutter, 1998; Bearse, Sutter, & Palmowski, 1997; Bearse, Sutter, Sim, & Stamper, 1996; Heinemann-Vernaleken, Palmowski, & Allgayer, 2000; Rudolph et al., 1998; Rudolph et al., 1998). In those studies some extent of a local glaucomatous damage could be measured with the mfERG, especially if the contrast of the multifocal display was reduced by 50% (Bearse & Sutter, 1998; Hood et al., 1999; Palmowski, Allgayer, & Heinemann-Vernaleken, 2000; Rudolph et al., 1998; Rudolph et al., 1998). However, only relatively subtle alterations were observed and no correlation to local visual field changes was found (Fortune et al., 2001; Hood et al., 2000; Sakemi et al., 2002). Unilateral visual field defects could not be detected reliably by the conventional mfERG (Fortune et al., 2001; Sakemi et al., 2002). In contrast, by using special multiflash stimulation a selective loss of an oscillatory component from the temporal retina could be proven (Fortune et al., 2002) and an area under the ROC curve of 0.88 was obtained. Such a technique could differentiate between normals and glaucoma eyes (Palmowski et al., 2002). Further improvement of isolating the optic nerve head component (ONHC) first proposed by Sutter and Bearse (1999) from the mfERG may further increase its diagnostic value.

4.7. Comparison to other methods

The best predictive parameter for the mfPERG was the difference P-50–N-95 which yielded 88% sensitivity with a specificity of 77%. This is as high as is claimed for most other new instruments designed specifically for glaucoma detection such as the frequency doubling technology (FDT) perimeter (Casson, James, Rubinstein, & Ali, 2001; Khong, Dimotrov, Rait, & McCarty, 2001). The ROC characteristics for the mfPERG are also comparable to established instruments such as the Heidelberg retina tomograph (HRT), the GDx nerve fiber analyzer and optical coherence tomography (OCT; Choplin & Lundy, 2001; Zangwill et al., 2001).

5. Conclusions

We found significant changes in the mfPERG of patients with glaucoma as compared to normal volunteers. The multi-input stimulation technique is robust with respect to simulation and malingering. We observed highly significantly decreased responses in all positive and negative components (P-50 and N-95) of the patients with glaucoma. However, those were most distinct in the central ring. Changes in latencies were not conclusive. Changes increase with a progression of glaucoma stage. A predictive model for detecting early glaucomatous changes was designed with high sensitivity and specificity. Thus the multifocal PERG may provide a useful tool in the diagnosis and the follow up of patients with glaucoma.

Acknowledgement

The authors thank Mrs. Christel Hörmann for expert technical assistance.

References

Asrani, S., Challa, P., Herndon, L., Lee, P., Stinnett, S., & Allingham, R. R. (2003). Correlation among retinal thickness, optic disc, and visual field in glaucoma patients and suspects: a pilot study. *Journal of Glaucoma, 12*, 119–128.

Aulhorn, E., & Karmeyer, H. (1977). Frequency distribution in early glaucomatous visual field defects. *Documenta Ophthalmologica, 44*, 75–83.

Bach, M. (2001). Electrophysiological approaches for early detection of glaucoma. *European Journal of Ophthalmology, 11*(Suppl. 2), S41–49.

Bach, M., Pfeiffer, N., & Birkner-Binder, D. (1993). In incipient glaucoma the pattern electroretinogram display diffuse retinal damage. *Ophthalmologe, 90*, 128–131.

Bach, M., Sulimma, F., & Gerling, J. (1997). Little correlation of the pattern electroretinogram (PERG) and visual field measures in early glaucoma. *Doccumenta Opthalmologica, 94*, 253–263.

Bayer, A. U., & Erb, C. (2002). Short wavelength automated perimetry, frequency doubling technology perimetry, and pattern electroretinography for prediction of progressive glaucomatous standard visual field defects. *Ophthalmology, 109*, 1009–1017.

Bayer, A. U., Maag, K. P., & Erb, C. (2002). Detection of optic neuropathy in glaucomatous eyes with normal standard visual

fields using a test battery of short-wavelength automated perimetry and pattern electroretinography. *Ophthalmology, 109*, 1350–1361.

Bearse, M. A., & Sutter, E. E. (1996). Imaging localized retinal dysfunction with the multifocal electroretinogram. *Journal of the Optical Society of America A, 13*, 634–640.

Bearse, M. A., & Sutter, E. E. (1998). Contrast dependence of multifocal ERG components. In *OSA Tech Dig Ser 1*, *Vision Science and its Applications* (pp. 24–27). Washington, DC: Optical Society of America.

Bearse, M. A., Sutter, E. E., & Palmowski, A. M. (1997). New development toward a clinical test of retinal ganglion cell function. In *OSA Tech Dig Ser 1*, *Vision Science and its Applications* (pp. 280–283). Washington, DC: Optical Society of America.

Bearse, M. A., Sutter, E. E., Sim, D., & Stamper, R. (1996). Glaucomatous dysfunction revealed in higher order components of the electroretinogram. In *OSA Tech Dig Ser 1*, *Vision Science and its Applications* (pp. 104–107). Washington, DC: Optical Society of America.

Berninger, T. A., & Arden, G. B. (1988). The pattern electroretinogram. *Eye, 2*(Suppl.), 257–283.

Casson, R., James, B., Rubinstein, A., & Ali, H. (2001). Clinical comparison of frequency doubling technology perimetry and Humphrey perimetry. *British Journal of Opthalmology, 85*, 360–362.

Chan, H. L., & Brown, B. (1999). Multifocal ERG changes in glaucoma. *Ophthalmic and Physiological Optics, 19*, 306–316.

Chan, H. H., & Brown, B. (2000). Pilot study of the multifocal electroretinogram in ocular hypertension. *British Journal of Opthalmology, 84*, 1147–1153.

Choplin, N. T., & Lundy, D. C. (2001). The sensitivity and specificity of scanning laser polarimetry in a detection of glaucoma in a clinical setting. *Ophthalmology, 108*, 899–904.

Curcio, C. A., Sloan, K. R., Jr., Packer, O., Hendrickson, A. E., & Kalina, R. E. (1987). Human photoreceptor topography. *Journal of Comparative Neurology, 292*, 497–523.

Esterberg, G. A. (1935). Topography of the layer of rods and cones in the human retina. *Acta Ophthalmologica, 13*(Suppl.), 1–102.

Fortune, B., Johnson, C. A., & Cioffi, G. A. (2001). The topographic relationship between multifocal electroretinographic and behavioral perimetric measures of function in glaucoma. *Optometry and Vision Science, 78*, 206–214.

Fortune, B., Bearse, M. A., Jr., Cioffi, G. A., & Johnson, C. A. (2002). Selective loss of an oscillatory component from temporal retinal multifocal ERG responses in glaucoma. *Investigative Ophthalmology & Visual Science, 43*, 2638–2647.

Graham, S. L., Drance, S. M., Chauhan, B. C., Swindale, N. V., Hnik, P., Mikelberg, F. S., & Douglas, G. R. (1996). Comparison of psychophysical and electrophysiological testing in early glaucoma. *Investigative Ophthalmology & Visual Science, 37*, 2651–2662.

Greenfield, D. S., Bagga, H., & Knighton, R. W. (2003). Macular thickness changes in glaucomatous optic neuropathy detected using optical coherence tomography. *Archives of Ophthalmology, 121*, 41–46.

Groneberg, A., & Treping, C. (1980). Topodiagnostik von Sehstörungen durch Ableitung retinaler und kortikaler Antworten auf Umkehr-Kontrastmuster. *Ber Dtsch Ophthalmol Ges, 77*, 409–417.

Guedes, V., Schuman, J. S., Hertzmark, E., Wollstein, G., Correnti, A., Mancini, R., Lederer, D., Voskanian, S., Velazquez, L., Pakter, H. M., Pedut-Kloizman, T., Fujimoto, J. G., & Mattox, C. (2003). Optical coherence tomography measurement of macular and nerve fiber layer thickness in normal and glaucomatous human eyes. *Ophthalmology, 110*, 177–189.

Hare, W. A., Ton, H., Ruiz, G., Feldmann, B., Wijono, M., & WoldeMussie, E. (2001). Characterization of retinal injury using ERG measures obtained with both conventional and multifocal methods in chronic ocular hypertensive primates. *Investigative Ophthalmology & Visual Science, 42*, 127–136.

Heinemann-Vernaleken, B., Palmowski, A., & Allgayer, R. (2000). The effect of time of day and repeat reliability on the fast flicker multifocal ERG. *Documenta Opthalmologica, 101*, 247–255.

Hess, R. F., & Baker, C. I. (1984). Human pattern-evoked elektroretinogramm. *Journal of Neurophysiology, 51*, 939–951.

Holder, G. E. (1987). Significance of abnormal pattern electroretinography in anterior visual pathway dysfunction. *British Journal of Ophthalmology, 71*, 166–171.

Holder, G. E. (2001). Pattern electroretinography (PERG) and an integrated approach to visual pathway diagnosis. *Progress in Retinal and Eye Research, 20*, 531–561.

Hollander, J., Bisti, S., Maffei, L., & Hebel, R. (1984). Electroretinographic responses and retrograde changes of retinal morphology after intracranial optic nerve section: a quantitative analysis in cat. *Experimental Brain Research, 55*, 483–493.

Hood, D. C., Greenstein, V., Fishman, L., Holopigian, K., Viswanathan, S., Seiple, W., Ahmed, J., & Robson, J. G. (1999). Identifying inner retinal contribution from action potentials to the primate multifocal ERG. In *OSA Tech Dig Ser 1*, *Vision Science and its Applications* (pp. 56–59). Washington, DC: Optical Society of America.

Hood, D. C., Greenstein, V. C., Holopigian, K., Bauer, R., Firoz, B., Liebmann, J. M., Odel, J. G., & Ritch, R. (2000). An attempt to detect glaucomatous damage to the inner retina with the multifocal ERG. *Investigative Ophthalmology & Visual Science, 41*, 1570–1579.

Kerrigan-Baumrind, L. A., Quigley, H. A., Pearse, M. E., Kerrigan, D. F., & Mitchell, R. S. (2000). Number of ganglion cells in glaucoma eyes compared with threshold visual field tests in the same persons. *Investigative Ophthalmology & Visual Science, 41*, 741–748.

Khong, J. J., Dimotrov, P. N., Rait, J., & McCarty, C. A. (2001). Can the specificity of the FDT for glaucoma be improved by confirming abnormal results. *Journal of Glaucoma, 10*, 199–202.

Klistorner, A. I., Graham, S. L., & Martins, A. (2000). Multifocal pattern electroretinogram does not demonstrate localized field defects in glaucoma. *Documenta Ophthalmologica, 100*, 155–166.

Korth, M. (1997). The value of electrophysiological testing in glaucomatous diseases. *Journal of Glaucoma, 6*, 331–343.

Korth, M., Horn, F., Strock, B., & Jonas, J. (1989). The pattern-evoked electroretinogram (PERG). Age-related alterations and changes in glaucoma. *Graefes Archive for Clinical and Experimental Ophtalmology, 227*, 123–130.

Kretschmann, U., Bock, M., Gockeln, R., & Zrenner, E. (2000). Clinical applications of multifocal electroretinography. *Documenta Ophthalmologica, 100*, 99–113.

Lindenberg, T., Horn, F., Rühl, S., & Korth, M. (2001). Multifokales ERG mit schnellem Musterwechsel bei glaukomatösen Gesichtsfeldausfällen. *Ophthalmologe, 98*(Suppl. 1), 111.

Maffei, L., & Fiorentini, A. (1981). Elektroretinographic response to alternating gratings before and after section of the optic nerve. *Science, 211*, 953–954.

Marx, M. S., Bodis-Wollner, I., Lustgarten, J. S., & Podos, S. (1988). Electrophysiological evidence that early glaucoma affects foveal vision. *Documenta Ophthalmologica, 7*, 281–301.

O'Donaghue, E., Arden, G. B., O'Sullivan, F., Falcao-Reis, F., Moriarty, B., Hitchings, R. A., Spilleers, W., Hogg, C., & Weinstein, G. (1992). The pattern electroretinogram in glaucoma and ocular hypertension. *British Journal of Opthalmology, 76*, 387–394.

Palmowski, A. M., Allgayer, R., & Heinemann-Vernaleken, B. (2000). The multifocal ERG in open angle glaucoma—a comparison of high and low contrast recordings in high- and low-tension open angle glaucoma. *Documenta Opthalmologica, 11*, 35–49.

Palmowski, A. M., Allgayer, R., Heinemann-Vernaleken, B., & Ruprecht, K. W. (2002). Multifocal electroretinogram with a multiflash stimulation technique in open-angle glaucoma. *Ophthalmic Research, 34*, 83–89.

Pfeiffer, N., Tillmon, B., & Bach, M. (1993). Predictive value of the pattern electroretinogram in high-risk ocular hypertension. *Investigative Ophthalmology & Visual Science, 34*, 1710–1715.

Raz, D., Seeliger, M. W., Geva, A. B., Percicot, C. L., Lambrou, G. N., & Ofri, R. (2002). The effect of contrast and luminance on mfERG responses in a monkey model of glaucoma. *Investigative Ophthalmology & Visual Science, 43*, 2027–2035.

Riggs, L. A., Johnson, E. P., & Schick, A. M. L. (1964). Electrical responses of the human eye to moving stimulus pattern. *Science, 144*, 567.

Rudolph, G., Bechmann, M., Berninger, T., Ehrt, O., Andrielis, H., Hörmann, C., Boergen, K. P., Schneider, A., & Kampik, A. (1998). Das Scanning Laser Ophthalmoskop evozierte multifokale ERG (SLO-m-ERG) in der Diagnostik hereditärer Augenerkrankungen. *Klin Mbl Augenheilkunde, 213*(Suppl. 2), 14.

Rudolph, G., Berninger, T., Arden, G. B., Bechmann, M., Zolnikova, I., Hörmann, C., & Kampik, A. (1998). Kartierung der retinalen Funktion mit dem multi-input Elektroretinogramm unter Anwendung einer neuen Technik. Das SLO evozierte multifocale ERG (SLO-m-ERG). *Ophthalmologe, 95*(Suppl. 1), 154.

Sakemi, F., Yoshii, M., & Okisaka, S. (2002). Multifocal electroretinograms in early primary open-angle glaucoma. *Japanese Journal of Ophthalmology, 46*, 443–450.

Salgarello, T., Colotto, A., Falsini, B., Buzzonetti, L., Cesari, L., Iarossi, G., & Scullica, L. (1999). Correlation of pattern electroretinogram with optic disc cup shape in ocular hypertension. *Investigative Ophthalmology & Visual Science, 40*, 1989–1997.

Shorstein, N. H., Dawson, W. W., & Sherwood, M. B. (1999). Mid-peripheral pattern electrical retinal responses in normals, glaucoma suspects, and glaucoma patients. *British Journal of Opthalmology, 83*, 15–23.

Sieving, P. A., & Steinberg, R. H. (1987). Proximal retinal contribution to the intraretinal 8-Hz-pattern ERG of cat. *Journal of Neurophysiology, 57*, 104–120.

Sutter, E. E., & Bearse, M. A. (1999). The optic nerve head component of the human ERG. *Vision Research, 39*, 419–436.

Sutter, E. E., & Tran, D. (1992). The field topography of ERG component in man—1: The photopic luminance response. *Vision Research, 32*, 433–446.

Vaegen, Anderton, P. J., & Millar, T. J. (2000). Multifocal, pattern and full field electroretinograms in cats with unilateral optic nerve section. *Documenta Ophthalmologica, 100*, 207–229.

Velten, I. M., Korth, M., & Horn, F. K. (2001). The a-wave of the dark adapted electroretinogram in glaucomas: are photoreceptors affected? *British Journal of Opthalmology, 85*, 397–402.

Viswanathan, S., Frishman, L. J., & Robson, J. G. (2000). The uniform field and pattern ERG in macaques with experimental glaucoma: removal of spiking activity. *Investigative Ophthalmology & Visual Science, 41*, 2797–2810.

Wassle, H., Grunert, U., Rohrenbeck, J., & Boycott, B. B. (1989). Cortical magnification factor and the ganglion cell density of the primate retina. *Nature, 341*, 643–646.

Weinstein, G. W., Arden, G. B., Hitchings, R. A., Ryan, S., Calthorpe, C. M., & Odom, J. V. (1988). The pattern electroretinogram (PERG) in ocular hypertension. *Archives of Ophthalmology, 16*, 923–931.

Zangwill, L. M., Bowd, C., Berry, C. C., Williams, J., Blumenthal, E. Z., Sanches, C. A., Vasile, C., & Weinreb, R. N. (2001). Discriminating between normal and glaucomatous eyes using heidelberg retina tomograph, GDx, nerve fiber analyser and coherence tomograph. *Archives of Ophtalmology, 119*, 985–993.

Zrenner, E., Baker, C. L., Hess, R. F., & Olsen, B. T. (1987). Die Lokalisation elektrographischer Antworten auf Musterumkehrreize und Helligkeitsreize in einzelnen Schichten der Primatennetzhaut. *Fortschritte Ophthalmology, 84*, 1605–1609.